The effect of pulsating pressure on the performance of a PEM fuel cell with a wavy cathode surface

Ashorynejad, Hamid Reza; Javaherdeh, Koroush; Van den Akker, Harry E.A.

DOI
10.1016/j.ijhydene.2016.05.291

Publication date
2016

Document Version
Accepted author manuscript

Published in
International Journal of Hydrogen Energy

Elsevier Editorial System(tm) for
International Journal of Hydrogen Energy
Manuscript Draft

Manuscript Number: HE-D-16-00302R1

Title: The effect of pulsating pressure on the performance of a PEM fuel cell with a wavy cathode surface

Article Type: Full Length Article

Section/Category: Fuel Cells & Applications

Keywords: PEM fuel cell; pressure pulsation; wavy wall; pore-scale modeling; heterogeneous GDL; lattice Boltzmann method

Corresponding Author: Dr. Hamid Reza Ashorynejad, Ph.D.

Corresponding Author's Institution: University of Guilan

First Author: Hamid Reza Ashorynejad, Ph.D.

Order of Authors: Hamid Reza Ashorynejad, Ph.D.; Koroush Javaherdeh, Ph.D.; Harry E.A. Van den Akker, Ph.D.

Abstract: In the context of attempts to improve the performance of Proton Exchange Membrane (PEM) fuel cells with a heterogeneous porous gas diffusion layer (GDL) consisting of carbon paper, we investigated whether - and to which degree - pulsating the pressure in a single waveform cathode channel affects the flow field in the channel and the performance of the fuel cell. In this 2-D study, the GDL was modeled by a stochastic arrangement of circular solid obstacles the macroscopic transport properties of which, such as permeability and tortuosity, were numerically simulated and found to compare favorably with experimental data. The focus of this paper is on the effects of varying amplitude and frequency of the pressure pulsations on cell performance. The results obtained show that a pulsating pressure enhances the convective species transport to the reaction sites and thereby increases cell performance. We found that in a waveform channel a pulsatile pressure with an amplitude as high as 0.7 times the pressure drop over the cathode channel improves the fuel cell performance by around 7%, while the effect of pulsation frequency on output power is marginally small only.

Cover letter

Dear **Professor N Veziroglu,**

I am submitting the below described manuscript for possible publication in the esteemed **International Journal of Hydrogen Energy.**

The submission is original, and is not being submitted for publication elsewhere.

- the article title:

The effect of pulsating pressure on the performance of a PEM fuel cell with a wavy cathode surface

- the full names of all authors:

Corresponding author: Hamid Reza Ashorynejad

Co-Authors: Koroush Javaherdeh, Harry E.A. Van den Akker

- the affiliation of authors:

Hamid Reza Ashorynejad , Faculty of Mechanical Engineering, Guilan University, Rasht, I. R. of Iran

Koroush Javaherdeh, Faculty of Mechanical Engineering, Guilan University, Rasht, I. R. of Iran

Harry E.A. Van den Akker, Faculty of Applied Sciences, Department of Chemical Engineering, Delft University of Technology, Netherlands

I thank you in advance and look forward to knowing about the status of manuscript.

Cordially Yours

Hamid Reza Ashorynejad
Ph.D Student
Faculty of Mechanical Engineering
University of Guilan
Rasht, Islamic Republic of Iran
Email: Ashorynejad@Phd.guilan.ac.ir & h.r.ashorynezhad@gmail.com
Web page : http://computer.guilan.ac.ir/phd/Ashorynejad/

***Detailed Response to Reviewers**

Click here to download Detailed Response to Reviewers: Response to reviews.docx

Response to Reviewers:

Reviewer #1: The paper represents an interesting contribution to the fuel cell research by proposing a model to understand the effect of pulsating pressure and frequency on PEM fuel cell performance. The paper is well written and the works seem to be original and very informative. Authors have done a very good job in including all the relevant information.

Authors are recommended to make some modifications to the paper according to the following comments.

1) Authors have proposed a model in this paper and matched it to the experimental data of Han. However, they never mentioned anything about how reliable is this model. There is no reliability study done to prove how accurately the model can predict the results over time and with different experimental conditions.

As you certainly know the polarization curve describes the performance of Fuel cell in the different current densities and when one simulation can predict the experimental data of polarization curve, it means this modeling is reliable. Also, the results of this model have been investigated with other experimental data in different operation condition and these results will be presented in another paper which is under publishing in one reputable journal.

2) What is the error percentage in predicting the results? There is no error estimating done in the results presented in this paper.

We added the error percentage on this paper.

3) Is there any design variability or exceptions in this model? Are there any cases where the model could not be used? Author needs to address that.

This model can be improved to multi-phase flow by adding interaction forces between the components. This single phase model can't well predict the flooding on the GDL and rapid decrease of performance of the fuel cell at high current density because of flooding. We try to extend this model to multi-phase in future works.

We have added one sentence at the end of conclusion to explain it.

4) The manuscript seems to be very lengthy. I would like them to make the manuscript more concise and shorten it.

We tried to present all detail of this modeling in shortest form but because of lot of details in this model, we can’t make shorter than this.

Reviewer #2: The paper is of interest as any idea to improve performance of PEMFC is to be discussed and models can help understanding its influence.

Some additional information are to be introduced before final acceptance.

1. Check that all the parameters are defined in the text

For instance, unless mistaken, nu (Eq. 1), (u,v) in Eq. (37) are not defined

We checked all equations and defined all parameters in equations.

2. Check that all the Eq. used in the text are the correct ones

For instance, reference to Eq. (28) should be Eq. (27)...

We have used an exponential function in eq.(27) for calculating ohmic resistance by using fitting parameters by own idea.

3. Some additional references would be useful, for instance:

* description of LBM (§2.1)

* Butler-Volmer Eq. (17)

We added the Refs.[25,30] for these sections.

4. Electrochemical model:

* the Butler-Volmer Eq (17) is surprising as no CH2O appears and CO2 is of a first order dependance ==> please justify and add a reference

The new novel half way bounce back boundary condition presented by Kamali et al. [29] was obtained by assumption of first order reaction on the catalyst layer. The ORR rate in PEMFCs is usually assumed to be first-order with respect to the oxygen concentration, indicating that the rate of oxygen consumption (and the current density) is proportional to the oxygen concentration at the catalyst sites. Based on this method was presented by Parthasarathy et al. (1992a) and they presented Tafel equation for modeling OOR in fuel cell and after that many researchers have used this model for modeling reaction on the catalyst layer. After some years the first-order Tafel equation was improved to Butler-Volmer equation presented by Madhusdana et al. (2007). Like most other modelers, Madhusdana et al. (2007) assumed that the ORR was first-order with respect to oxygen concentration. In this study we used this model for reaction. We have added the Ref.[30] for Butler-Volmer equation.

* the Vcell (Eq. 26) does neglect mass transport, whereas the paper deals with influence of gas transport ==> please justify

The values of eta and I completely depend to the concentration of Oxygen on the surface of catalyst layer. Thus V_cell depends to mass transport. I have added one sentence after Eq.(26) to explain it.

5. Topics that are unclear to me and shall be more explained* unless mistaken, you simulate gas permeability and gas diffusion ==> if so, can you conclude on which of these transfers the pulsating gas has more influence?

In this paper, first the ability of this method for modeling flow on the heterogeneous porous media with one suggested geometry (an overlapping random distribution of circular obstacles) was compared with previous studies. For this comparison, we investigated the effective parameters in characterizing porous media such as permeability and tortuosity. Our computational results first of all showed that our way of mimicking the porous GDL reproduces several (semi-)empirical correlations available in the literature. After that we used this structure for GDL in PEMFC and investigated the overall performance of PEM in different conditions and we didn't separately investigate the gas permeability and gas diffusion for PEMFC in pulsating condition. "One may expect that the positive effect of pulsatile flow may mainly be due to increased species transport in the open channel, as the transport in the GDL may be affected to a much lesser extent due to the limited permeability." We added this sentence above Fig. 12 in the paper.

* Eq (18) deals with the influence of liquid saturation; it seems that this relates to the cathode catalyst layer (CCL), but the CCL seems to be a surface condition ==> please explain how you simulate the CCL

There are two different ways for simulating the CCL. One way is modeling volumetric catalyst layer and solve momentum and mass transfer equations on it. In the second way the narrow catalyst layer predicts as a surface and only the boundary conditions implement on it. In this paper we used second way. The liquid saturation can calculate by eq.(18) for all domains but we used only its value on the surface of catalyst layer in eq.(17). These values estimate the liquid saturation on the catalyst layer in the second way.

We have modified first paragraph of section 2.2.1 to explain it on the paper.

* Pv(T) used in Eq (19) is at operating conditions ==> why don't you consider the local conditions, at CCL interface

We assumed that the channel is isothermal, so the temperature of flow and water vapor saturation pressure in all domains is fixed. Because of P_v only depends to temperature. We have modified 3rd assumption in section 3.

* the "top surface" on which Eq (20) are applied is not clear on the figures

The top surface in this sentence indicates to CCL and we showed it on fig. 1.

* I would expect that the study could also have been done with more classical approaches (continuous using Darcy equation) ==> please explain the advantages/drawbacks of LBM compared to the other approaches

LBM can easily simulate the flow through complex geometries and porous media such as this heterogeneous GDL which was considered in this study because of using simple bounce back boundary condition on the surface of solid walls and also this presented model was used modified bounce back boundary condition where it needs only one node on the reactive surface which is very easy to implement. The LBM code can be easily parallelized because the collision is calculated locally. The extension of this model to 3D with real geometry in the GDL is easy although that is computationally expensive.

* "p13 "As a result... numerically" ==> please explain this sentence, what would be the other choices than modeling and experiments?

Of course there isn't another choice. The structure of this sentence has been changed in final version.

* §2.4.1: LBM is performed on a random solid structure

==> how do you manage the "real" Pore Size Distribution of the GDL?

==> do you perform statistical analysis on the spatial distribution of the fibers? If no what difference would you expect? If yes, what is the standard deviation? Please also discuss this in the frame of the comparison Fig.3. is this comparison a function of this spatial distribution hypothesis?

In this study, the obstacles diameter and porosity of GDL and overlapping random distribution of obstacles have been adjusted. The different distributions such as staggered parallel fiber

geometry and quadratic fiber distribution were investigated and by comparison with previous studied we found this distribution can well predict the permeability and tortuosity of GDL. There are some empirical correlations for calculating permeability and tortuosity as a function of porosity and Fig. 3 revealed our numerical results in comparison of these empirical correlations. We found our result has a good agreement with empirical data.

* the anisotropy of GDL is to be discussed in Eq (32) and (33); could you compare the LBM anisotropy to these?

Exactly in Fig. 3 the LBM results compared with TS model (Eq.32) and TS model (Eq.33).

* §3: assumption (2): is laminar still valid in the case of wavy channels studied?

Yes, The Reynolds Number on the wavy channels is under 10, thus the laminar flow is valid for this range of Reynolds.

* §3: assumption (4): why this hypothesis? Could we use more realistic dependencies?

The First-order reaction is very common on the catalyst layer and the boundary conditions on catalyst surface in Eqs. (20-21) were obtained by this assumption. It needs to more fundamental study to obtain the LBM B.C from more realistic B.C.

* §4.1: comparison is done on Ref [5] from Han ==> are the GDL, Operating Conditions the same in both cases?

The pressure and temperature operating conditions and other geometrical parameters in this study is the same as Han’s study [5].

* §4.2: the channel waves enhance the transport of species: does this depend on the flow field design on the anode side?

We assumed that the enough hydrogen protons and electron exist on the cathode catalyst layer and only with more diffusion of Oxygen in the cathode GDL, the reaction rate on the catalyst layer enhances. Absolutely, in real case the design of flow field of anode effects on the performance of PEMFC. However splitting of the hydrogen molecule is relatively easier than oxygen molecule, thus the cathode side design is more effective on the performance of PEMFC.

* §4.2: the maximum velocity is two times higher in the case of straight channel; what about the average velocity? Is the increase of performance linked to the increased maximum or increased average?

The time average velocity and stoichiometry ratio of inlet air is constant in all cases of this study. But increasing of maximum velocity can enhance the performance of fuel cell.

* §4.3: please add the values of deltaP (in mbar for instance) and not only in dimensionnel form

We have corrected them.

* Fig 1: add the cathode active layer

We have added it to Fig 1.

* Fig 2: the GDL structure is 3D with fibers perpendicular to the Fig ==> please discuss the relevance of the 2D-model

Transport phenomena in some structures can be efficiently modeled in 2D with significant computational savings and without compromising accuracy. Perpendicular flow over arrays of infinite parallel fibers is an example of a 2D simulation that is representative of the 3D case. However, there are situations where 3D modeling is required, such as when the geometry and flow fields are not symmetric. In this study, we assumed all parallel fibers perpendicular to xy plate which can be accurately modeled in 2D.

* Fig. 3: are experimental results included in the comparison? If no, please compare for instance to the data sheet of the manufacturer

The present LBM results were compared with the experimental data which was presented by Han et. al [5] in Fig.5.

Highlights research

The active approach pore-scale LBM was used for PEMFC simulation.

The GDL was modeled by a stochastic arrangement of circular solid obstacles.

The waveform channel with pulsatile pressure improves the fuel cell performance around 7%.

The effect of pulsating pressure on the performance of a PEM fuel cell with a wavy cathode surface

Hamid Reza Ashorynejad[1]
Faculty of Mechanical Engineering, Guilan University, Rasht, I. R. of Iran
Email: ashorynejad@phd.guilan.ac.ir

Koroush Javaherdeh
Faculty of Mechanical Engineering, Guilan University, Rasht, I. R. of Iran
Email: javaherdeh@guilan.ac.ir

Harry E.A. Van den Akker
Faculty of Applied Sciences, Department of Chemical Engineering,
Delft University of Technology, Netherlands
Email: h.e.a.vandenakker@tudelft.nl

Abstract:

In the context of attempts to improve the performance of Proton Exchange Membrane (PEM) fuel cells with a heterogeneous porous gas diffusion layer (GDL) consisting of carbon paper, we investigated whether - and to which degree - pulsating the pressure in a single waveform cathode channel affects the flow field in the channel and the performance of the fuel cell. In this 2-D study, the GDL was modeled by a stochastic arrangement of circular solid obstacles the macroscopic transport properties of which, such as permeability and tortuosity, were numerically simulated and found to compare favorably with experimental data. The focus of this paper is on the effects of varying amplitude and frequency of the pressure pulsations on cell performance. The results obtained show that a pulsating pressure enhances the convective species transport to the reaction sites and thereby increases cell performance. We found that in a waveform channel a pulsatile pressure with an amplitude as high as 0.7 times the pressure drop over the cathode channel improves the fuel cell performance by around 7%, while the effect of pulsation frequency on output power is marginally small only.

[1] **Corresponding Author:** Hamid Reza Ashorynejad, Faculty of Mechanical Engineering, Guilan University, Rasht, I. R. of Iran, Tel: +981316690528 Ext 3109, POB: 41635-3756
E-mail addresses : ashorynejad@phd.guilan.ac.ir , h.r.ashorynezhad@gmail.com

Keywords: *PEM fuel cell, pressure pulsation, wavy wall, pore-scale modeling, heterogeneous GDL, lattice Boltzmann method*

1. Introduction

In a fuel cell, the chemical energy stored in fuels is directly converted into electricity power; the efficiency of this process is relatively high, e.g. with respect to heat engines [1]. Due to its low operating temperature, very low emissions and – in principle - high power density, the Proton Exchange Membrane Fuel Cell (PEMFC) looks very attractive as a power source for future automotive and portable applications. The size of the fuel cell is a decisive issue for portable applications: the smaller the more attractive but also the more difficult to remedy certain drawbacks.

Particularly in many of the smaller devices, and depending on the ambient operating conditions, the output power density of this type of fuel cell suffers from a low diffusion flux of oxygen (air) and from flooding by the water produced [6]. Imposing a forced convective flow with the help of a blower or compressor may cure the issue of mass transfer limitation. Several investigators tried to improve the performance of a PEMFC even further. Kuo and Chen [2-4] proposed a waveform cathode surface and claimed that this novelty improved the power density delivered by the fuel cell by almost 40 % [4]. Recent experimental data reported by Han et al. [5], however, did not confirm this claim. Han et al. [5] investigated the effect of a wavy channel wall in a PEMFC both numerically and experimentally, and found the fuel cell's performance improved by just some 5%. Their results further indicated that the optimum value for the Expansion Ratio (ER) is two, where ER is defined as the ratio of channel depth to the wave's amplitude. Another option to reduce serious power loss while keeping system size small is by means of a pulsating or oscillating air flow [7].

This paper investigates the combined effect of an oscillating air flow and a wavy cathode surface on the performance of a PEMFC. The geometry investigated is shown in Figure 1.

Figure 1

There are several studies about the effect of oscillations on mass transfer in straight and waveform channels. Nishimura and Kojima [8] experimentally studied the effects of pulsating flow on the mass-transfer in a symmetrical sinusoidal wavy-walled channel. They showed that the combination of flow separation and oscillation leads to a significant increase in mass transfer rates under laminar-flow conditions. In another study, Nishimura et al. [9] experimentally investigated the influence of an oscillation frequency on mass transfer in grooved channels at a high Schmidt number. They found that intermediate Strouhal numbers resulted in substantial transport enhancement in laminar flows.

There are just a few reports, however, on applying oscillating air flow in fuel cells. Hwang et al. [7] experimentally studied the oxygen diffusion rate at the cathode of PEMFC in a pure oscillating flow (the mean flow rate being zero) and measured the effects of oscillation frequency f and sweep distance (oscillation amplitude). The effect of the frequency was expressed in terms of the non-dimensional Womersley number α defined by

$$\alpha = H_c \sqrt{\pi f / 2\upsilon} \tag{1}$$

in which H_c stands for the channel height and υ is the kinematic viscosity. According to Hwang et al. [7], the reaction rate of the oxygen increases linearly with sweep distance, while the non-dimensional effective diffusivity varies linearly with α for $\alpha >> 1$. Recently, Ramiar et al. [10] numerically studied the effect of pulsation of the air flow at the cathode side of a PEMFC with an interdigitated flow field by using a transient 2-D isothermal two-phase multi-component transport model. They found that the pulsation amplitude increased the fuel cell performance

while the pulsation frequency didn't have a significant effect. To the best of the authors' knowledge, the effect of air pulsation in a waveform cathode channel in PEMFC has never been studied before.

In all of these numerical studies, the porous medium of the cathode electrode, i.e. the gas diffusion layer (GDL), is considered homogeneous and isotropic with uniform morphological properties such as porosity, tortuosity and permeability. In reality, however, GDLs are inhomogeneous and anisotropic [11], since in general they are fabricated from carbon fiber based paper or cloth. The microscopic structure of a GDL may significantly influence the performance of a PEMFC. The real microstructure of the cathode electrode porous medium may be mimicked by means of pore-scale numerical tools among which the Lattice Boltzmann (LB) methods seem very attractive [12].

In fact, LB has superior properties as to dealing with a domain with a complicated morphology, parallelization of the algorithm, and modeling multi-phase fluid flow with a dynamic interface in a porous medium [13]. Classical chemical engineering models fall short due to the use of empirical correlations incapable of distinguishing between the transport of the various species. Although several studies modelled specific phenomena in a fuel cell such as the water management [14-17], the structure of the GDL [18-20] and the reactive flow in a porous medium [21,22] by means of LBM, just a few studies adopted LB methods to investigate the flow in all different layers of a fuel cell and its effect on the cell performance [23,24].

In the present study, the Pseudo-Potential LB method originally proposed by Shan and Chen [25] has been used for simulating multicomponent and transport processes in a 2-D PEMFC. Rather than using an approach in which the mixture behavior is the starting point, we used the so-called 'active approach' in which the coupled velocity and concentration fields of each individual

species are solved. In this approach, the mutual interactions of all components are much more accurately taken into account. Recently, this model was also used by Molaeimanesh et al. [26-28] for simulating a PEMFC with interdigitated flow field. Another advantage of this approach is that the modified bounce back rule proposed by Kamali et al. [29] for the reaction surface can easily be incorporated.

The purpose of the present study is to investigate the effect of a pulsating air pressure in a waveform cathode channel of PEMFC while considering a pore-scale model for the GDL and to explore the effects of both pulsation amplitude and pulsating frequency on the fuel cell performance. The focus of this paper is on the cathode side as its lay-out seems to have the biggest impact on the performance of a fuel cell, the hydrogen conversion at the anode being less critical.

2. Numerical approach:

2.1. Single-phase Multicomponent LBM

The general form of the lattice Boltzmann equation for a distribution function f_i^k in the so-called BGK approximation is [25]:

$$f_i^k(x+\vec{e}_i\Delta t, t+\Delta t) = \omega_k f_{i,k}^{eq}(x,t) + [1-\omega_k] f_i^k(x,t) \qquad (2)$$

Here, the superscript k denotes the kth chemical species and the subscript i denotes the velocity direction of a single particle, $\omega_k = 1/\tau_k$ where τ_k is the single relaxation time for each component that relates to the kinematic viscosity ν_k for each species and which is defined as:

$$\tau_k = \left(3\frac{\Delta t}{\Delta x^2}\nu_k + 0.5 \right) \tag{3}$$

The particle streaming velocity ($\vec{e}_i$) for the usual D2Q9 model is defined as:

$$\vec{e}_i = \begin{cases} (0,0) & i = 0 \\ (\cos[(i-1)\pi/2], \sin[(i-1)\pi/2]) \cdot c & i = 1,2,3,4 \\ \sqrt{2}(\cos[(i-5)\pi/2 + \pi/4], \sin[(i-5)\pi/2 + \pi/4]) \cdot c & i = 5,6,7,8 \end{cases} \tag{4}$$

where $c = \Delta x / \Delta t$ is the lattice speed set equal to unity. In eq. (2), $f_{i,k}^{eq}$ denotes the local equilibrium distribution function is defined as [25]:

$$f_{i,k}^{eq} = \rho_k w_i \left[1 + \frac{\vec{e}_i \cdot \vec{u'}}{c_S^2} + \frac{1}{2}\frac{(\vec{e}_i \cdot \vec{u'})^2}{c_S^4} - \frac{1}{2}\frac{\vec{u'}^2}{c_S^2} \right] \qquad i = 0,...,8 \tag{5}$$

where $\vec{u'}$ is the common velocity in lattice units, ρ_k is the component density, w_i is the weight function, which has the values of $w_0 = 4/9$, $w_i = 1/9$ for $i = 1$ to 4, and $w_i = 1/36$ for $i = 5$ to 8and $c_S = c/\sqrt{3}$ is the speed of sound.

To implement the Pseudo-Potential model originally proposed by Shan and Chen [25] for the single-phase multicomponent flow comprising the three species, viz. oxygen, nitrogen and water vapor, the streaming and collision steps are solved individually for each species to find all distribution functions f_i^k. The component density and velocity are then defined as follows:

$$\rho_k = \sum_i f_i^k \tag{6}$$

$$\vec{u}_k = \frac{\sum_i f_i^k \vec{e}_i}{\rho_k} \tag{7}$$

and total density and common velocity are obtained [25]:

$$\rho_{total} = \sum_k \rho_k \tag{8}$$

$$\vec{u'} = \frac{\sum_k \sum_i f_i^{\,k} \vec{e}_i \omega_k}{\sum_k \omega_k \rho_k} \tag{9}$$

Also, the mass fraction of each component is obtained by:

$$Y_k = \frac{\rho_k}{\rho_{total}} \tag{10}$$

We assume that all species obey the ideal gas law. Therefore, the total concentration is obtained by:

$$C_{total} = \frac{P}{RT} \tag{11}$$

where P and T are operating pressure and temperature of the fuel cell.

For calculating the mole fraction of species, at first, we need to obtain the mixture molecular weight for each domain with mass fraction and molecular weight of species:

$$M_{Mix} = \left(\sum_k \frac{Y_k}{M_k} \right)^{-1} \tag{12}$$

Now, the mole fraction and the concentration of species k are calculated by:

$$X_k = M_{mix} \frac{Y_k}{M_k} \tag{13}$$

$$C_k = X_k C_{total} \tag{14}$$

2.2 Boundary conditions

2.2.1 The reactive surface

The cathode catalyst layer (CCL) is not explicitly modelled in our approach; rather, it is conceived as the boundary condition for the computational domain. At the surface of this CCL, we adopt the novel half-way bounce back boundary condition for multi-component LBM on a no slip wall with surface reaction as recently proposed by Kamali et al. [29].

In this approach, it is needed to calculate the dimensionless surface reaction constant in the LB context from the real-world surface reaction constant K_s and the real-world diffusion coefficient D_A as follows:

$$K_s^{LB} = \frac{\left(6K_s \frac{\Delta t}{\Delta x}\right)}{\left(1+\frac{K_s \Delta x}{2D_A}\right)} \tag{15}$$

After calculating K_s^{LB}, it is easy to derive the halfway bounce-back boundary condition that simulates a surface reaction; for instance, in a PEMFC, oxygen reacts to water on the cathode surface of catalyst layer above of the GDL:

$$O_2 + 4H^+ + 4e^- \rightarrow 2H_2O$$

The real-world surface reaction constant K_s is related to the electrical current density I that is generated from the reaction according to

$$K_s = \frac{I}{4F\,C_{O_2}} \tag{16}$$

where F is Faraday's constant and C_{O_2} is the oxygen concentration on the surface of the cathode.

The current density I follows from the Butler-Volmer equation [30]:

$$I = \frac{a^{eff} I_0 (1-s)}{C_{O_2}^{ref}} C_{O_2} \left(\exp(\frac{\alpha_c F \eta_c}{RT}) - \exp(-\frac{\alpha_a F \eta_c}{RT}) \right) \quad (17)$$

where I_0 is a reference current density, $C_{O_2}^{ref}$ is a reference oxygen concentration, α_c and α_a are cathode and anode mass transfer coefficients, η_c is the activation loss, R is the universal gas constant and T is the operating temperature. In Eq. (17), a^{eff} is the roughness factor the value of which is chosen by fitting the model to experimental data [5]. The values of these parameters are all listed in Tables 1 and 2.

Although single-phase modeling is the starting-point in this study, in real life the cathode reaction suffers from the formation of liquid water. The factor $(1-s)$ in Eq. (17) is a correction factor accounting for the reduced number of active reaction sites easily accessible for oxygen as a result of the formation of liquid water [31, 32]. Here, s denotes the liquid water saturation which can be calculated from:

$$s = \frac{\rho_L \left(Y^w - Y_{sat}^w \right)}{\rho_L \left(1 - Y^w \right) + \rho_g \left(Y^w - Y_{sat}^w \right)} \quad (18)$$

where ρ_L and ρ_g denote the densities of liquid water and air, respectively, while Y^w and Y_{sat}^w represent the mass fractions of water vapor and saturated vapor, respectively; Y_{sat}^w is defined as:

$$Y_{sat}^w = \frac{M_w P_v(T)}{R \rho_g T} \quad (19)$$

where $P_v(T)$ is water vapor saturation pressure at the operating temperature. The unknown distribution functions for each species on the CCL are calculated as follows:

for oxygen:

$$f_4^{O_2} = (1-k_s^{LB}) f_2^{O_2}$$

$$f_7^{O_2} = (1-k_s^{LB}) f_5^{O_2} \quad (20)$$

$$f_8^{O_2} = (1-k_s^{LB}) f_6^{O_2}$$

and for water:

$$f_4^{H_2O} = (1+2\alpha_w)\frac{2M_{H_2O}}{M_{O_2}} k_s^{LB} f_2^{O_2} - f_2^{H_2O}$$

$$f_7^{H_2O} = (1+2\alpha_w)\frac{2M_{H_2O}}{M_{O_2}} k_s^{LB} f_5^{O_2} - f_5^{H_2O} \quad (21)$$

$$f_8^{H_2O} = (1+2\alpha_w)\frac{2M_{H_2O}}{M_{O_2}} k_s^{LB} f_6^{O_2} - f_6^{H_2O}$$

where M_k denotes the molecular mass of species k and α_w is the net water transport coefficient.

As a result of the water production at the catalyst layer, water might travel from anode to cathode through the membrane. This water transfer may be due to three effects, viz., electro-osmotic drag (number of water molecules carried by each proton), back diffusion (due to the different water concentrations at anode and cathode) and water transfer by convection due to the pressure difference between anode and cathode. All three mechanisms are condensed into the mass transfer coefficient α_w in the water vapor boundary condition which reflects the number of water molecules transported per proton. This coefficient has been used in previous numerical studies [33-34].

2.2.2 Inlet and Outlet Boundary Condition

First, the total density at the inlet is obtained by the ideal gas law from the (fluctuating) inlet pressure. The inlet mass fraction of each species multiplied with the total density then gives the (fluctuating) density of each species. Finally, the inlet velocities for the different species are calculated by the Zou and He method [35]:

$$\rho_{total} = \frac{P_{in}}{3} \tag{22}$$

$$\rho_k = Y_k \, \rho_{total} \tag{23}$$

$$u_k = 1 - \frac{f_0^k + f_2^k + f_4^k + 2(f_3^k + f_6^k + f_7^k)}{\rho_k} \tag{24}$$

The unknown distribution functions at the inlet are obtained from:

$$\begin{aligned} f_1^k &= f_3^k + \frac{2}{3}\rho_k u_k \\ f_5^k &= f_7^k + \frac{1}{2}\left(f_4^k - f_2^k\right) + \frac{1}{6}\rho_k u_k \\ f_8^k &= f_6^k + \frac{1}{2}\left(f_2^k - f_4^k\right) + \frac{1}{6}\rho_k u_k \end{aligned} \tag{25}$$

The same approach with constant ambient pressure is used for the outlet boundary condition. Because of the zero concentration gradient in the outlet of channel, the density of each component is calculated by using the mass fraction of species at the upstream nodes. The stability of this boundary condition, along with its independency of viscosity (or relaxation time), is the big advantage beyond the more common LBM open boundary condition such as the extrapolation method and the Neumann boundary condition.

Since the Knudsen number for the gas in the channel and in the GDL is in the order of 10^{-2}, the fluid may be regarded as a continuum. Thus, implementing no-slip boundary conditions with the

help of a bounce-back rule is justified on any solid wall in the GDL as well as on the wavy wall. Similarly, it is allowed to adopt the method proposed in [36-37] for dealing with velocity components at curved boundaries.

2.3 Potential and current density:

The performance of a PEMFC is usually expressed in terms of a polarization curve that relates the cell potential V_{cell} to the current density I (in A/m^2) and which can be calculated from [38]:

$$V_{cell} = E_{oc} - \eta_c - R_{ohm} I \qquad (26)$$

in which E_{oc} denotes the open circuit potential, η_c represents the activation loss, and R_{ohm} stands for the total internal resistance of the PEMFC. The various losses will be explained briefly below. Note that both the current density and the activation loss, and therefore also V_{cell}, depend on the rate the oxygen reaches the catalytic surface of the cathode.

The total internal resistance R_{ohm} comprises the electronic resistance (which usually is very small), the ionic resistance, and the contact resistance at the interface between the bipolar plates and the gas diffusion layers. The ionic resistance on the membrane increases with increasing current density due to dry-out of the membrane on the anode side. In the present work, the internal resistance is approximated by means of an exponential function:

$$R_{ohm} = A + B e^{CI} \qquad (27)$$

in which the constants A, B and C are parameters the values of which will be chosen by fitting the model to experimental data (see Section 4.1 and Figure 4).

In Eq.(26), E_{oc} is the open circuit potential defined by Mann et al. [39]:

$$E_{oc} = E_{rev} - E_{mix} \tag{28}$$

where E_{rev} denotes the reversible cell potential which depends on the cell temperature and the partial pressure of oxygen and hydrogen; it is defined by a modified version of the Nernst equation [39] as:

$$E_{rev} = 1.185 - 2.302\times10^{-4}(T - 298.15) + 4.308\times10^{-5}T\ln\left(\frac{X_{H_2O}}{X_{H_2}X_{O_2}^{0.5}}\right) - 2.154\times10^{-5}T\ln\left(\frac{P_{ref}}{P}\right) \tag{29}$$

in which X_k is the mole fraction of component *k*.

In Eq. (28), E_{mix} is the mixed potential between the electrodes which might be due to such effects as the crossover of fuel through the electrolyte from anode to cathode or vice versa, slow O_2-reduction kinetics, Pt-oxide formation, and oxidation of impurities [40-41].

2.4. Structure of the GDL

2.4.1 The representation of the GDL

Generally, GDLs in PEMFCs are porous media made of carbon fibers 7-10 μm in diameter, assembled in the form of papers or cloths [42]. These materials have a complex microstructure with a random distribution of fibers which does not allow for an exact representation of flow field and permeability. In this regard, some researchers experimentally and numerically investigated flow in porous media to determine the permeability of GDLs as a function of porosity. We opted for mimicking the GDL by means of a random arrangement of cylindrical obstructions 10 μm in diameter which may touch upon each other. This 3-D structure was then

simplified to a random 2-D structure of circles, which were approximated by means of octagons with mesh size much smaller than the octagon size (see Figure 2). Typical values for porosity, fiber diameter and thickness of a GDL were selected from a common type of GDL, viz. the commercial brand TGP-H-120 the properties of which were reported by the manufacturer and by Gostick et al. [42].

Figure 2

To show the power of LBM for modeling the fluid flow in such a random structure mimicking a porous medium, we will compare our LBM results for permeability and tortuosity with previous empirical and analytical equations specified below.

2.4.2 Permeability:

The permeability and its relation with porosity are effective parameters in characterizing porous media. The permeability K (in m^2) of a porous medium is numerically calculated from Darcy's law [43]:

$$K = -\frac{\mu \langle u \rangle}{\nabla P} \tag{30}$$

where $\langle u \rangle$ denotes the volume-averaged flow velocity, μ is the dynamic viscosity of the fluid and ∇P represents the pressure gradient. Eq. (30) is valid for incompressible steady single-phase low Reynolds number flows and constant fluid properties. The Reynolds number based on the fiber diameter is lower than 0.1 in the present study; therefore, the Darcy equation is applicable.

Gebart [44] performed a combined theoretical, numerical, and experimental study of the permeability of ordered arrays of fibers and presented the following permeability-porosity relation in the limit of closely packed fibers:

$$\frac{K}{R^2} = C_G \left[\sqrt{\frac{1-\varepsilon_c}{1-\varepsilon}} - 1 \right]^{2.5} \tag{31}$$

where R denotes fiber radius, ε is porosity, and ε_c is the critical porosity below which flow does not occur (i.e. percolation threshold). C_G is a proportionality constant, also known as the geometric factor, for which Gebart found $C_G = \frac{16}{9\pi\sqrt{2}}$ while $\varepsilon_c = 1 - \frac{\pi}{4}$ for a square arrangement. Gebart [44] showed that the above analytically determined permeability is in agreement with a finite difference solution of the NS equations for porosity values up to 0.65.

Gostick et al. [42] report a relation due to Tomadakis and Sotirchos (TS) predicting the anisotropic permeability of 1-D, 2-D and 3-D random fiber beds which only requires fiber diameter and porosity as input parameters. The TS expression for the absolute permeability runs as:

$$\frac{K}{R^2} = \frac{\varepsilon\,(\varepsilon - \varepsilon_p)^{(2+\alpha)}}{8\,(ln\,\varepsilon)^2 (1-\varepsilon_p)^{\alpha} \left[(1+\alpha)\,\varepsilon - \varepsilon_p \right]^2} \tag{32}$$

where ε_p and α are fitting parameters which depend on the geometry of the fibrous structure. For a 2-D random alignment of fibers, which is analogous to the carbon fiber structure in a conventional carbon paper GDL, ε_p is set to 0.11 while α is set to 0.785.

Tamayol and Bahrami (TB) [45-46] used a scaling analysis to relate the permeability of a fibrous medium to its microstructure and geometrical parameters such as tortuosity, pore diameter and porosity. They successfully compared their model (TB) – see eq. (33) – with experimental data collected from various sources for a variety of materials:

$$\frac{K}{R^2} = 0.048(1-\varphi)\left[\left(\frac{\pi}{4\varphi}\right)^2 - \frac{\pi}{2\varphi} + 1\right]\left[1 + 0.72\frac{\varphi}{(0.89-\varphi)^{0.54}}\right] \qquad (33)$$

where φ denotes the solids volume fraction, i.e., $\varphi = 1-\varepsilon$. With a view to our current case of interest, their model is able to demonstrate the effects of the compression factor H_G/H_{comp} where H_G and H_{comp} denote the compressed and uncompressed GDL thicknesses, respectively, viz. by recalculating the solid volume fraction and porosity by means of [19]:

$$\varphi_{comp} = \varphi_0 \frac{H_G}{H_{comp}} \qquad (34)$$

Finally, when polytetrafluoroethylene (PTFE) is added onto the carbon paper GDL, the pore volume may be randomly filled with PTFE. According to Hao and Cheng [19], the final porosity, ε_{PTFE}, can be expressed in terms of the PTFE content, ω, and the original porosity ε_0:

$$\varepsilon_{PTFE} = \varepsilon_0 - 0.9\frac{\omega(1-\varepsilon_0)}{(1-\omega)} \qquad (35)$$

Eqs. (34-35) will be used to transform the porosity of a fresh GDL to the value under live conditions in a PEMFC to be used in the simulations.

2.4.3 Tortuosity:

Another important feature of porous media is tortuosity which is defined as the ratio of the actual path length in the porous medium as covered by the fluid particles to the shortest distance in the direction of the flow:

$$\tau = \frac{L_{\text{Actual}}}{L_{\text{Shortest}}} \tag{36}$$

The volume averaged tortuosity in the streamwise direction (i.e., the x-direction) can be calculated from [20]:

$$\tau = \frac{\sum \sqrt{u^2 + v^2}}{\sum |u|} \tag{37}$$

Koponen et al. [47] studied 2-D random porous media by using lattice gas automata (LGA) and arrived at the following correlation for tortuosity as a function of porosity:

$$\tau = 1 + a\,\frac{1-\varepsilon}{(\varepsilon - \varepsilon_c)^m} \tag{38}$$

where a, m and ε_c are fitting parameters equal to 0.19, 0.65 and 0.33, respectively.

2.5 A pulsating pressure

In this paper, pressure at the inlet is pulsating according to:

$$P_{in} = P_{op} + \Delta P\,(1 + Amp \times \sin(2\pi\, ft)) \tag{39}$$

in which P_{op} is the operating pressure, ΔP is the average pressure difference between inlet and outlet, f is the frequency of the pulsation, and Amp denotes a non-dimensional pulsation amplitude.

A main element of this paper relates to the effect of a pulsating pressure on the performance of a PEMFC. The effect of the frequency of such pulsations is investigated in terms of the

Womersley number α – see Eq. (1) – varying between 0.5 and 2, while *Amp* is varied in the range between 0.1 and 0.7. The pressure difference between inlet and outlet in this equation is considered $\Delta P = 0.03$ mbar for the waveform channel.

In general, the pulsatile pressure at the inlet of the channel leads to fluctuations in the output averaged current density along the time. The time averaged current density is calculated according to:

$$I_{time-ave} = \frac{\int_0^T I_{ave} dt}{T} \tag{40}$$

3. Details of the simulations

The simulations are about 2-D single-phase multi-component isothermal flow in a PEMFC cathode channel including a porous GDL consisting of fibers 10 μm in average diameter. The simulations were carried out to validate the concept of a random 2-D structure of circles mimicking the fibrous GDL structure and to investigate the effects of a wavy channel wall and a pulsating pressure on the performance of PEMFCs. The geometries studied are shown in Figs. 1 and 2. For the bottom of the channel, a sinusoidal wavy wall is considered with amplitude H_w and wave length L, where $H_w = H_c/2$ and $L = 4H_w$ to allow for comparison with results reported by Han et al. [5].

The following assumptions are considered for the simulations:

(1) Ideal gas law is employed for gaseous species.

(2) The fluid flow in the fuel cell is laminar due to the low flow velocities and the small size of channel.

(3) The fuel cell cooling is controlled by forced convection heat transfer and the temperature in the channel is assumed to be uniform and constant.

(4) The reaction occurring in the catalyst layer is first-order, meaning that the local oxygen consumption rate is linearly proportional to its concentration.

The computational domain comprises both the cathode channel and the GDL with different rectangular meshes for these two zones. A coarse mesh $4000\,\Delta x_c \times 100\,\Delta x_c$ is used for the open cathode domain, whereas a fine mesh $16000\,\Delta x_f \times 120\,\Delta x_f$ is used for the porous GDL with $\Delta x_c = 10\ \mu m$ and $\Delta x_f = 2.5\ \mu m$, respectively. To enable such a local mesh refinement in the LBM, the speed of sound and the kinematic viscosity should be equivalent on all sub-grids to guarantee physical consistency. According to Filippova and Hanel [48], the refinement factor $m_r = \Delta x_c / \Delta x_f = 4$ requires $\Delta t_c / \Delta t_f = 4$ where the subscripts c and f still relate to the coarse and the fine grid, respectively. Consequently, the relaxation parameters should also be rescaled such that the kinematic viscosity is the same on both grids:

$$\tau_f = m_r\,(\tau_c - \frac{1}{2}) + \frac{1}{2} \tag{41}$$

For more details on mesh refinement in the LBM, the reader is referred to refs. [49-50].

To study the effects of the key parameters of pulsating flow, i.e., the amplitude and the frequency, on the performance of a PEMFC, a transient simulation is needed. Along with the fine lattice used for the GDL sub-domain (needed to accurately resolve the flow between solid obstacles), this would lead to excessive running times. To mitigate this issue, the channel length for the base validation is taken equal to 4 cm, while in the remainder of this study it was reduced by a factor of 2, to 2 cm.

The compression factor and the PTFE content for the carbon paper GDL of the commercial brand TGP-H-120 used for this study amount to 1.2 and 15%, respectively, where the original porosity equals to 0.79. By substituting these values into Eqs. (34) and (35), a final porosity of 0.7 is obtained that was used in our simulations.

Tables 1 and 2 present the numerical values of physical properties, operating conditions and geometrical parameters used throughout all our simulations.

Table 1

Table 2

4. Results and discussions

4.1 The base case including our 2-D pore scale modeling

First, in the absence of a chemical reaction, we investigated whether our pore scale modeling illustrated in Fig. 2 was capable of mimicking permeability and tortuosity of real-life porous media. Fig.3(a) shows a comparison between our LBM results and some empirical relations from literature for permeability and tortuosity in the porosity range 0.65 – 0.85 which is common for a GDL in a PEMFC.

A close agreement is observed between our LBM results and the various permeability–porosity relationships. Also, the tortuosity calculated by Eq. (37) on the basis of our LBM data compares favorably with Koponen's correlation in Fig.3(b). The maximum error of permeability between LBM result and TB model is under 3% and for tortuosity is near 2% .We conclude that our pore-scale LBM is a powerful tool for simulating the porous GDL of a PEMFC.

Figure 3

Figure 4

In the next step, the cell performance of a regular PEMFC (with a single straight cathode channel) was evaluated. To this end, a series of LB simulations were carried out in which the activation loss was increased stepwise from 0.1 to 0.4 with the view of increasing the surface reaction constant – see Eqs. (16) and (17). Each of these simulations results in values for the oxygen concentration at the cathode surface and the water saturation *s*; by using these values, a series of potential and current density are calculated with the view of constructing the pertinent polarization curve. In this procedure, we need values for the parameters A, B and C in Eq. (28) for the ohmic resistance of the fuel cell. Figure 4 presents the various potential losses in the fuel cell as a function of the current density. The ohmic loss is described by means of an exponential function as expressed in Eq. (28). By using such a function rather than a fixed value, and by optimizing the values of A, B and C in Eq. (28) we obtained fuel cell potentials comparable with those reported by Han et al .[5], especially at high current densities. Fig. 5 then presents a comparison of our eventual results with the experimental data reported by Han et al. [5].

It is noteworthy that our simulation can accurately predict the performance of the PEMFC even in the high current density, where the maximum error of 4% occurs in this area. The maximum power density occurs at a current density of about 1.2 A/cm^2 where the activation loss amounts to 0.365 V and the total ohmic loss is about 0.215 V, the cell potential is around 0.44 V and, consequently, the maximum power density is almost 0.525 W/cm^2.

Figure 5

Since the optimized parameters A, B and C are related to losses concentrated in the upper layers of the cathode GDL, such as the membrane and the anode catalyst layer, it is rather safe to use

these values in the remainder of this study that focuses on flow and transport phenomena in the cathode channel as a result of a waveform channel bottom and pulsatile pressures.

4.2 A PEMFC with a waveform channel

The idea behind a waveform channel is that the periodic expansions and contractions of the channel width assist the transport of species towards and from the cathode. Fig. 6 presents the axial velocity fields in both the straight and the wavy channel.

Figure 6

Figure 7

In general, the velocity increases along the channel, because the reaction of oxygen with hydrogen on the catalytic cathode surface produces water (vapor plus liquid) that is transported into the cathode channel. As a result, the flux at the outlet of the cathode channel will be larger than the flux at the inlet. In the waveform channel, velocities are locally higher than in the straight channel because half of the channel's cross-sectional area is occupied by wavy wall. Consequently, the maximum velocity in our waveform channel is roughly two times higher than in our straight channel.

Fig. 7 shows the velocity field and the stream lines in the middle plane of the GDL in the straight channel as well as above the middle crest in the waveform channel at high power density. Our results show that the maximum velocities in the narrow regions between the circular obstacles are significantly higher in the wavy channel, especially near the interface of GDL and channel.

Figure 8

Fig. 8 shows the effect of the waveform channel in comparison with the straight channel without pulsating flow: the maximum power density increases from 0.525 W/cm^2 in the straight channel to 0.55 W/cm^2 in the waveform channel at a cell potential of about 0.44 V. The wavy wall doesn't have a significant effect, however, on the performance of a fuel cell at low current densities. The wavy channel is found to improve the maximum power density by just some 5% , in excellent agreement with experimental data reported by Han et al. [5].

4.3 A PEMFC with a pulsating pressure

Fig. 9 presents how the output current density reaches a steady pattern after a number of pressure pulsations and illustrates the effect of varying the Womersley number α at a constant pulsation amplitude Amp =0.5 and at the maximum power density for a cell potential of about 0.44 V. The amplitude of the fluctuations in the output current density decreases for increasing α , a higher α means a higher frequency which leaves the oxygen insufficient time to penetrate in the GDL and to affect the reaction rate on the catalyst surface. As a result, at α = 2, the output current density fluctuates by just 0.2% between 12525 to 12555 A/m^2. At lower α values, however, the output current densities oscillate significantly: at α = 0.5, the fluctuations in the output current density amount to some 6.5% between 12200 to 13000 A/m^2.

Figure 9

For all the above cases in which only the effect of α was investigated, the time averaged current density increased by some 6% in comparison with the straight reference channel. This increase hardly depends on α¸ all averaged values (the dashed lines) approaching a similar value after some cycles.

The effect of the non-dimensional pulsation amplitude *Amp* at a fixed Womersley number α =1 is presented in Fig. 10. Increasing the pulsation amplitude not only increases the fluctuations of the output current density, but also the time average current density (represented by the dashed lines): increasing *Amp* from 0.1 to 0.5 increases the time average current density from 12420 to 12550 A/m^2, i.e. by 1%.

Figure 10

Figure 11

The above results suggest that the performance of fuel cells can be improved by applying higher frequencies and larger amplitudes for the pulsating flow. Fig. 11 then presents the effect of pulsation amplitude *Amp* in the range 0.5 – 0.7 on the polarization curve at α =2 where the latter value has been chosen to avoid too strong fluctuations in the output current density. The results show the maximum power density is approximately 0.555 W/cm^2 for *Amp* = 0.6 and 0.7 whereas this value is about 0.52 W/cm^2 in the straight reference channel, while this higher value is obtained at a higher current density.

The overall conclusion of the simulations is that the performance of a PEMFC can be improved by some 7% by using pulsatile flow in a waveform channel provided that higher values for the Womersley number α and the pulsation amplitude *Amp* are used. These findings deserve a more in-depth analysis and explanation in terms of velocity and concentration fields.

Fig. 12 shows the contours of the axial velocity along the channel at different time steps within a pulsation period of duration *T*, for α = 2 and *Amp* = 0.7. At $t = T/4$, both pressure and axial velocity are maximum at the inlet, since for $\alpha < 3$ pressure and velocity are in phase. This maximum propagates through the channel; at $t = T/2$, it has arrived in the second half of the

channel, while at this moment the inlet pressure is 0.03 mbar higher than the outlet pressure and the velocity at the inlet is around 0.12 m/s. Finally, at time of t = 3T/4, the inlet pressure is minimum (just 0.009 mbar higher than at the outlet) leading to a dramatic reduction of the inlet velocity: it drops to below 0.04 m/s while at this moment the average outlet velocity is higher than some 0.2 m/s. This means there is a substantial active breathing effect. One may expect that the positive effect of pulsatile flow may mainly be due to increased species transport in the open channel, as the transport in the GDL may be affected to a much lesser extent due to the limited permeability.

Figure 12

Fig. 13 displays a number of concentration fields in the case of maximum power density for pulsatile pressure with α = 2 and Amp = 0.7 at $T = T/2$. Figure 13(a) shows how overall the oxygen mass fraction along the channel decreases along the channel. Thanks to the diffusion of oxygen into the GDL and the reaction on the catalyst surface, water vapor is produced, resulting in an increase of the water mass fraction along the channel: Fig. 13(b) shows how the water vapor mass fraction increases from 0.06 at the inlet (at an imposed relative humidity of 70%) to around 0.22 at the outlet of the channel. As can be inferred from Fig. 13(c), water saturation also increases along the channel because of its direct relation with the water vapor mass fraction as expressed by Eq. (18) in which the value of Y_{sat}^{w} calculated with the help of Eq. (19) amounts to 0.076 for the operating condition pertinent to this simulation.

Figure 13

The production of water deserves some further comments. As soon as the water vapor mass fraction rises above the critical value Y_{sat}^{w}, liquid water may be produced. In our simulations, the

effect of liquid water on flooding the GDL is only considered in an empirical way by the effect of water saturation on the Butler-Volmer equation, see Eq. (17). A more sophisticated approach of the water production requires a multiphase model which is the topic of future research. In real life, the pulsating flow may help to remove the produced water from the GDL and enhance the performance of the fuel cell even further.

5. Conclusions

In this study on PEMFCs, the effect of a pulsating pressure on their performance was investigated for cells with a waveform cathode channel. This was done by carrying out 2-D Lattice Boltzmann simulations of single-phase multi-component flow of oxygen, nitrogen and water vapor through a cathode channel including a heterogeneous porous gas diffusion layer (GDL). The chemical reaction at the cathode was modelled by means of the half-way bounce-back rule proposed by Kamali et al. [29]. The relevant result of each simulation is the oxygen concentration at the cathode surface and the water saturation s from which the current density is calculated with the help of the Butler-Volmer equation. By varying stepwise the activation loss, which affects the surface reaction constant and therefore oxygen concentration as well as water saturation, the so-called polarization curves are obtained which relate cell potential to current density. The heterogeneous GDL was mimicked by an overlapping random distribution of circular obstacles, while in the majority of the simulations the cathode channel had a wavy bottom. The effect of pressure pulsations was evaluated for different values of the Womersley number α (denoting the non-dimensional pulsation frequency) and the amplitude of the pulsations. A stoichiometric ratio of 1.5 was used throughout. The effect of the formation of liquid water was taken into account by means of a correction factor in the Butler-Volmer equation.

Our computational results first of all showed that our way of mimicking the porous GDL reproduces several (semi-)empirical correlations available in the literature for permeability and tortuosity. Secondly, our simulations were able to reproduce typical polarization curves such as those reported by Han et al. [5], thanks to the use of some fitting parameters for the cell's internal resistance and roughness. Then, the effect of switching to a waveform cathode channel was investigated.

The main conclusions of the paper relate to the effect of pulsating pressure in a waveform channel: the maximum power density improves by some 7% by applying a pulsating pressure at the inlet of a waveform channel at a Womersley number α of 2 and a non-dimensional pulsation amplitude *Amp* of 0.7. Our simulations demonstrate the effects of the waveform channel and the pressure pulsations on the flow and concentration fields in the GDL and in the channel. Their combined effects result in spatially and temporally varying velocities and concentrations which assist in increasing the oxygen transport toward the cathode surface. The effect of water production and flooding has been taken into account by means of an empirical correction coefficient and should be described better with the help of a more sophisticated version of the Pseudo-Potential Lattice Boltzmann model that allows for the formation of a liquid phase.

References:

[1] Yang TH, Park G, Pugazhendhi P, Lee WY, Kim CS. Performance Improvement of Electrode for PEM Fuel Cell. Korean J. Chem. Eng. 2002; 19 (3):417-420.

[2] Kuo JK, Yen TH, Chen CK. Three-dimensional numerical analysis of PEM fuel cells with straight and wave-like gas flow fields channel. J. Power Sources 2008; 177:96-103.

[3] Kuo JK, Chen CK. Evaluating the enhanced performance of a novel wave-like form gas flow channel in the PEMFC using the field synergy principle. J. Power Sources 2006; 162:1122-9.

[4] Kuo JK, Chen CK. The effects of buoyancy on the performance of a PEM fuel cell with a wave-like gas flow channel design by numerical investigation. Int. J. Heat and Mass Transfer 2007; 50:4166–4179.

[5] Han SH, Choi NH, Choi YD. Simulation and experimental analysis on the performance of PEM fuel cell by the wave-like surface design at the cathode channel. Int. J. Hydrogen Energy 2014; 39:2628-2638.

[6] Chu D, Jiang RZ. Performance of polymer electrolyte membrane fuel cell (PEMFC) stacks. J. Power Sources 1999; 83:128–133.

[7] Hwang YS, Lee DY, Choi JW, Kim SY, Cho SH, Joonho P , Kim MS, Jang JH, Kim SH, Cha SW. Enhanced diffusion in polymer electrolyte membrane fuel cells using oscillation, Int. J. Hydrogen Energy 2010; 35:3676-3683.

[8] Nishimura T, Kojima N. Mass transfer enhancement in a symmetric sinusoidal wavy-walled channel for pulsatile flow. Int. J. Heat and Mass Transfer 1995; 38:1719–31.

[9] Nishimura T, Oka N, Yoshinaka Y, Kunitsugu K. Influence of imposed oscillatory frequency on mass transfer enhancement of grooved channels for pulsatile flow. Int. J. Heat Mass Transfer 2000; 43:2365–74.

[10] Ramiar A, Mahmoudi AH, Esmaili Q, Abdollahzadeh M. Influence of cathode flow pulsation on performance of proton exchange membrane fuel cell with interdigitated gas distributors. Energy 2016; 94:206-217.

[11] Ostadi H, Rama P, Liu Y, Chen R, Zhang X, Jiang K. Nanotomography based study of gas diffusion layers. Microelectron Eng. 2010; 87:1640-1642.

[12] Kim KN, Kang JH, Lee SG, Nam JH, Kim CJ. Lattice Boltzmann simulation of liquid water transport in microporous and gas diffusion layers of polymer electrolyte membrane fuel cells. J. of Power Sources 2015; 278:703-717.

[13] Chen S, Doolen GD. Lattice Boltzmann method for fluid flows. Annu. Rev. Fluid Mech. 1998; 30:329-64.

[14] Han B, Meng H. Numerical studies of interfacial phenomena in liquid water transport in polymer electrolyte membrane fuel cells using the lattice Boltzmann method. Int. J. Hydrogen Energy 2013; 38:5053-5059.

[15] Hao L, Cheng P. Lattice Boltzmann simulations of water transport in gas diffusion layer of a polymer electrolyte membrane fuel cell. J. of Power Sources 2010; 195:3870-3881.

[16] Ben Amara MEA, Ben Nasrallah S. Numerical simulation of droplet dynamics in a proton exchange membrane (PEMFC) fuel cell micro-channel. Int. J. Hydrogen Energy 2015; 40:1333-1342.

[17] Molaeimanesh GR, Akbari MH. Impact of PTFE distribution on the removal of liquid water from a PEMFC electrode by lattice Boltzmann. Int. J. Hydrogen Energy 2014; 39(16):8401-8409.

[18] Park J, Matsubara M, Li X. Application of lattice Boltzmann method to a micro-scale flow simulation in the porous electrode of a PEM fuel cell. J. of Power Sources 2007; 173:404-414.

[19] Hao L, Cheng P. Lattice Boltzmann simulations of anisotropic permeability in carbon paper gas diffusion layers. J. of Power Sources 2009; 186:104-114.

[20] Khabbazi EA, Ellis JS, Bazylak A. Developing a new form of the Kozeny–Carman parameter for structured porous media through lattice-Boltzmann modeling, Computers & Fluids 2013; 75:35–41.

[21] Kang Q, Lichtner PC, Janecky DR. Lattice Boltzmann Method for Reacting Flows in Porous Media. Advances in Applied Mathematics and Mechanics 2010; 2(5):545-563.

[22] Chen L, Kang Q, He YL, Tao WQ. Pore-scale simulation of coupled multiple physicochemical thermal processes in micro reactor for hydrogen production using lattice Boltzmann method. Int. J. Hydrogen Energy 2012; 37:13943–13957.

[23] Aghajani Delavar M, Farhadi M, Sedighi K. Numerical simulation of direct methanol fuel cells using lattice Boltzmann method, Int. J. Hydrogen Energy 2010; 35: 9306–9317.

[24] Chen L, Luan HB, He YL, Tao WQ. Pore-scale flow and mass transport in gas diffusion layer of proton exchange membrane fuel cell with interdigitated flow fields. Int. J. Thermal Sciences 2012; 51:132-144.

[25] Shan X, Chen H. Lattice Boltzmann model for simulating flows with multiple phases and components. Phys. Rev. E 1993; 47:1815-1820.

[26] Molaeimanesh GR, Akbari MH. A three-dimensional pore-scale model of the cathode electrode in polymer-electrolyte membrane fuel cell by lattice Boltzmann method. J. of Power Sources 2014; 258:89-97.

[27] Molaeimanesh GR, Akbari MH. A pore-scale model for the cathode electrode of a proton exchange membrane fuel cell by lattice Boltzmann method. Korean J. Chem. Eng. 2015; 32(3): 397-405.

[28] Molaeimanesh GR, Akbari MH. Agglomerate modeling of cathode catalyst layer of a PEM fuel cell by the lattice Boltzmann method. Int. J. Hydrogen Energy 2015; 40(15):5169-5185.

[29] Kamali MR, Sundaresan S, Van den Akker HEA, Gillissen JJJ. A multi-component two-phase lattice Boltzmann method applied to a 1-D Fischer-Tropsch reactor. Chem. Eng. J. 2012; 207-208:587-95.

[30] Mench MM. Fuel cell engines. 1st ed. New Jersey: John Wiley & Sons; 2008.

[31] Natarajan D, Van Nguyen T. A two-dimensional two-phase multicomponent transient model for the cathode of a proton exchange membrane fuel cell using conventional gas. J. Electrochem. Soc. 2001; 148 (12): A1324-1335.

[32] Wang ZH, Wang CY, Chen K.S. Two-phase flow and transport in the air cathode of proton exchange membrane fuel cells. J. of Power Sources 2001; 94:40-50.

[33] Van Nguyen T, White RE, Water A. Heat management model for proton exchange membrane fuel cells. J. Electrochem. Soc. 1993; 140(8):2178–2186.

[34] Liu X, Tao W, Li Z, He Y. Three-dimensional transport model of PEM fuel cell with straight flow channels, J of Power Sources 2006; 158:25–35.

[35] Zou Q, He X. On pressure and velocity boundary conditions for the lattice Boltzmann BGK model. Phys. Fluids 1997; 9:1591-1598.

[36] Filippova O, Hanel D. Grid refinement for lattice-BGK models. Comp. Phys. 1998; 147:219-228.

[37] Mei R, Yu D, Shyy W, Luo LSH. Force evaluation in the lattice Boltzmann method involving curved geometry. Phys. Rev. E 2002; 65:1-14.

[38] Barbir F, PEM fuel cells: theory and practice. San Diego: Academic Press; 2005.

[39] Mann RF, Amphlett JC, Hooper MAI, Jensen HM, Peppley BA, Roberge PR, Development and application of a generalised steady-state electrochemical model for a PEM fuel cell. J. Power Sources 2000; 86(1–2):173–80.

[40] Eikerling M, Kornyshev AA, Kuznetsov AM, Ulstrup J, Walbran S. Mechanisms of Proton Conductance in Polymer Electrolyte Membranes. J. Phys. Chem. B 2001; 105: 3646- 3662.

[41] Das PK, Xianguo L, Zhong-Sheng L. Analytical approach to PEM fuel cell performance and optimization. J. Electroanalytical Chemistry 2007; 604:72–90.

[42] Gostick JT, Fowler MW, Pritzker MD, Ioannidis MA, Behra L.M. In-plane and through-plane gas permeability of carbon fiber electrode backing layers, J. Power Sources 2006; 162(1): 228-238.

[43] Kaviany M. Principles of Heat Transfer in Porous Media. 2nd ed. New York; Springer Verlag:1995.

[44] Gebart B.R. Permeability of unidirectional reinforcements for RTM. J. Compos. Mater. 1992; 26(8):1100–1133.

[45] Tamayol A, Bahrami M, Transverse permeability of fibrous porous media. Phys. Rev. E 2010; 83:046314.

[46] Tamayol A, McGregor F, Bahrami M. Through-Plane Gas Permeability of Proton Exchange Membrane Fuel Cell Gas Diffusion Layers. Proceedings of 5th Int'l Conference on Energy Sustainability & 9th Fuel Cell Science, Engineering and Technology Conference, ASME2011, August 7-10, 2011, Washington, DC, USA

[47] Koponen A, Kataja M, Timonen J. Permeability and effective porosity of porous media. Phys. Rev. E 1997; 56(3):3319-3325.

[48] Filippova O, Hanel D. Boundary-fitting and local grid refinement for lattice-BGK models. Int. J. Modern Physics C 1998; 9(8):1271-1279.

[49] Meng J, Zhang Y, Shan X. Multiscale lattice Boltzmann approach to modeling gas flows. Phys. Rev. E 2011; 83(4): 046701.

[50] Kandhai D, Soll W, Chen S, Hoekstra A, Sloot P. Finite-Difference Lattice-BGK methods on nested grids. Computer Physics Communications 2000; 129(1–3):100–109.

Table

Table 1. Physical parameters and operating conditions

Parameter	Symbol	Value
Operating temperature	T	323 (K)
Operating pressure	P	1 (bar)
Faraday's constant	F	96485 ($\mathrm{C\,mol^{-1}}$)
Universal gas constant	R	8.314 ($\mathrm{J\,mol^{-1}K^{-1}}$)
Water vapor dynamic viscosity	μ_w	$4.11\times10^{-3}\left(\frac{T}{291.15}\right)^{1.5}(T+120)^{-1}$ ($\mathrm{kg\,m^{-1}s^{-1}}$)
Oxygen dynamic viscosity	μ_{O_2}	$8.46\times10^{-3}\left(\frac{T}{292.15}\right)^{1.5}(T+127)^{-1}$ ($\mathrm{kg\,m^{-1}s^{-1}}$)
Nitrogen dynamic viscosity	μ_{N_2}	$7.33\times10^{-3}\left(\frac{T}{300.55}\right)^{1.5}(T+111)^{-1}$ ($\mathrm{kg\,m^{-1}s^{-1}}$)
Oxygen diffusivity	D_{O_2}	$2.2\times10^{-5}\left(\frac{T}{293}\right)^{1.5}\left(\frac{1}{P}\right)$ ($\mathrm{m^2s^{-1}}$) [34]
Reference current density	I_0	1.3874×10^{-2} ($\mathrm{A\,m^{-2}}$) [26]
Reference oxygen concentration	$C_{O_2}^{ref}$	10.875 ($\mathrm{mol\,m^{-3}}$) [17]
Cathode transfer coefficient	α_c	0.5 [26]
Anode transfer coefficient	α_a	1 [26]
Net water transport coefficient	α_w	0.3
Roughness factor	a^{eff}	3000
Fitting parameters	A, B, C	0.16 ($\Omega\,\mathrm{m^2}$), 4×10^{-4} ($\Omega\,\mathrm{m^2}$), 5×10^{-5} ($\mathrm{A^{-1}\,m^2}$)
Mixed potential	E_{mix}	0.16 (V) [41]

Table 2. Geometry parameters

Parameter	Symbol	Value
Channel length	L_c	2×10^{-2} (m)
Channel height	H_c	10×10^{-4} (m)
GDL height	H_G	3×10^{-4} (m)
Amplitude of wave	H_w	5×10^{-4} (m)
Wavelength	L	2×10^{-3} (m)
GDL porosity	ε	0.70
Relative humidity at the inlet	RH	70 (%)
Stoichiometry ratio of oxygen	λ	1.5
Mass fraction of oxygen	Y_{O_2}	0.22
Mass fraction of water vapor	Y_w	0.055
Mass fraction of nitrogen	Y_{N_2}	0.725

Figure

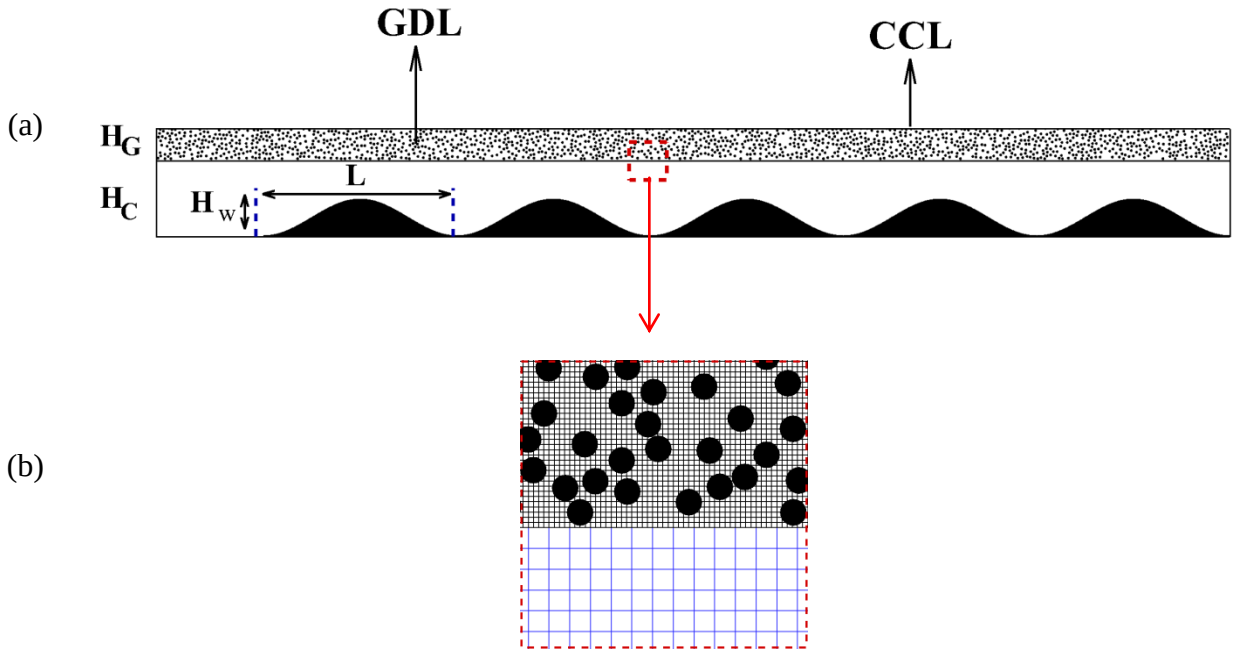

Fig. 1. (a) Computational domain of a PEMFC wavy cathode channel; (b) the structure of the mesh on the specified zone at the interface of channel and GDL

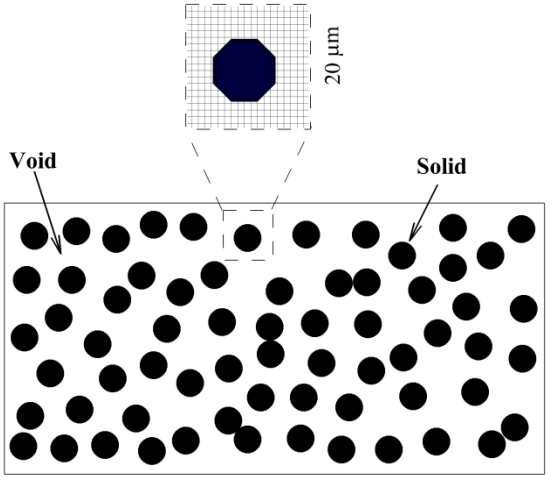

Fig. 2. Representation of the random arrangement of parallel fibers by means of a 2-D arrangement of circles with the cross-sectional areas of the fibers in black. Each circle is approximated by means of an octagon.

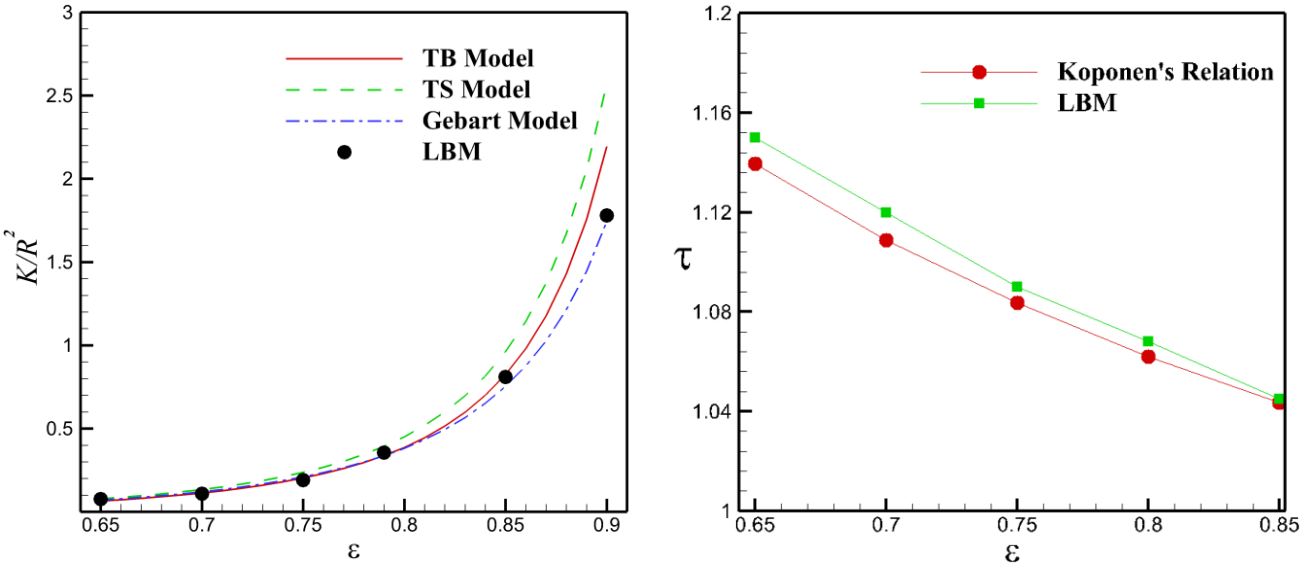

(a) (b)

Fig. 3. Comparison of our LBM results for (a) the non-dimensional permeability with Gebart's analytical relation [44], the TS model [42] and the TB model [46]; for (b) tortuosity with Koponen's correlation [47].

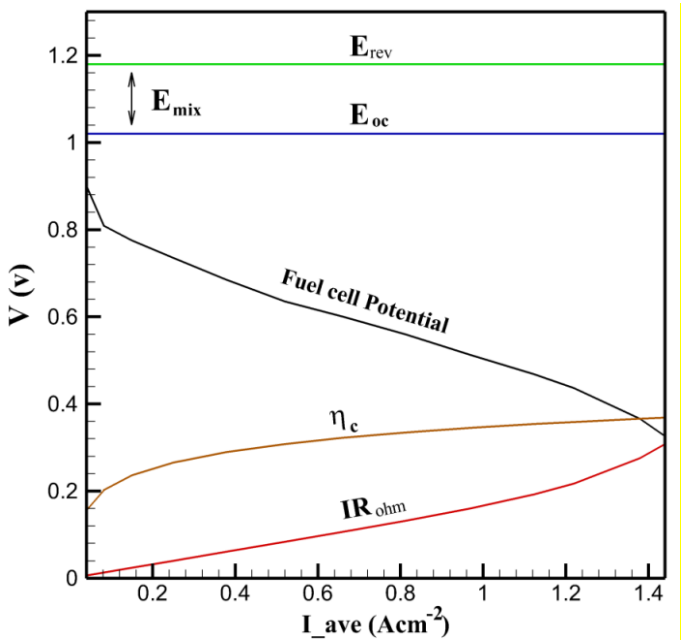

Fig. 4. Various losses of fuel cell potential in the validation case

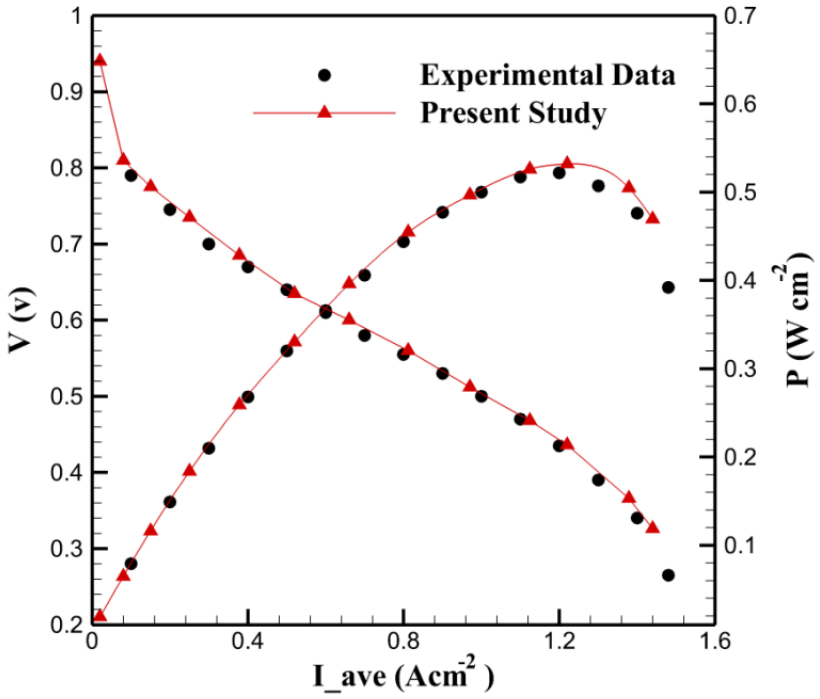

Fig. 5. The comparison between the present modeling (solid line) with experiments (dots) by Han et al.[5].

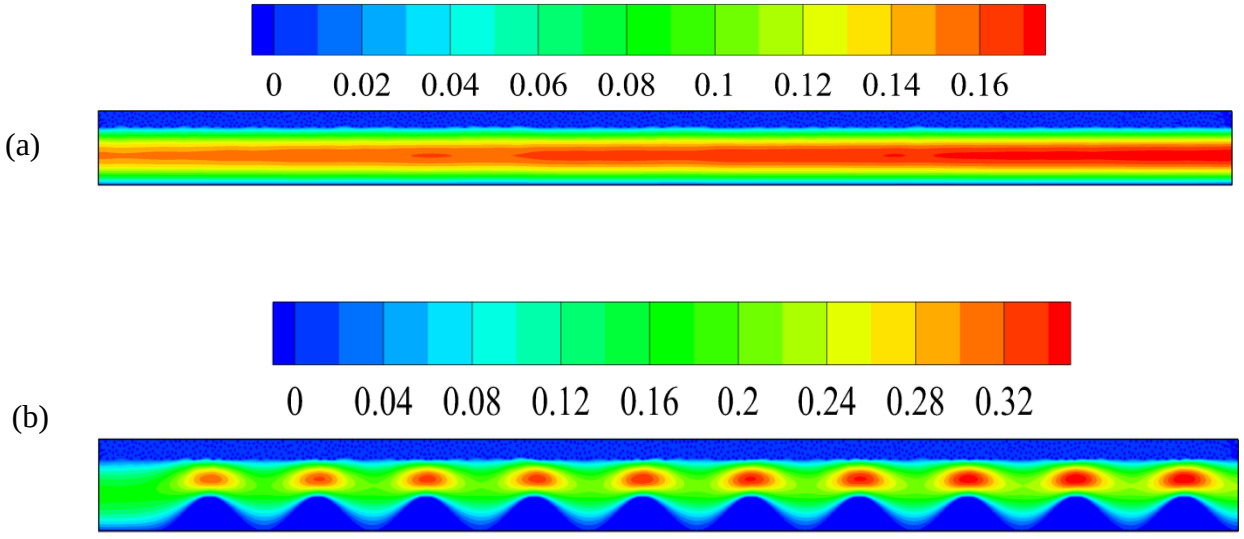

Fig. 6. The axial velocity fields in the straight and waveform channels at the maximum current density

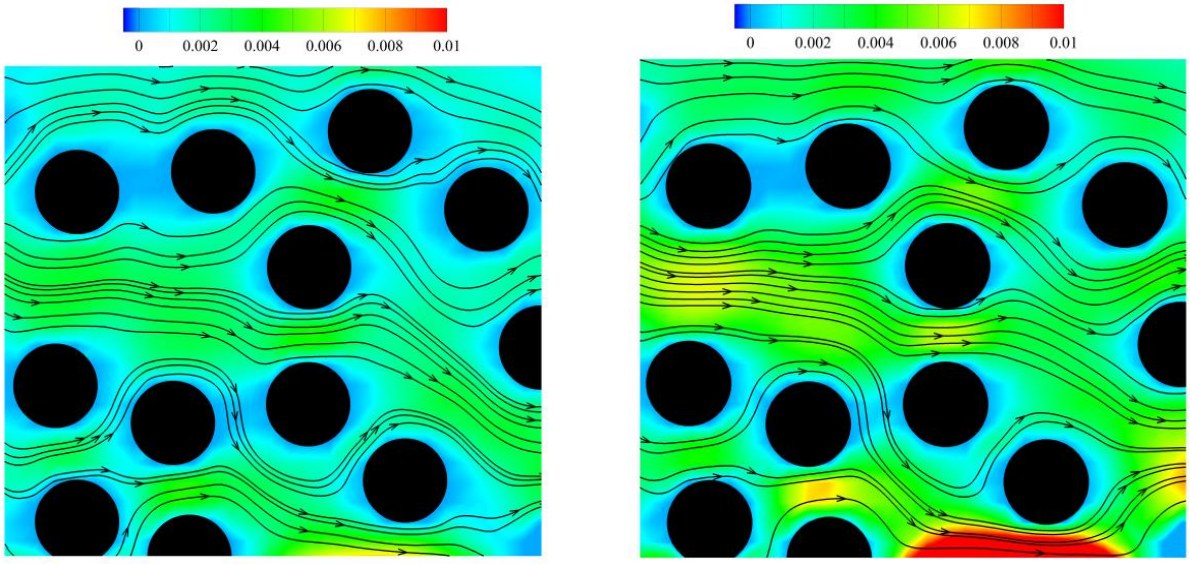

(a) (b)

Fig. 7. Velocity contours and streamlines in the middle of a GDL in (a) a straight channel and in (b) a waveform channel at maximum current density

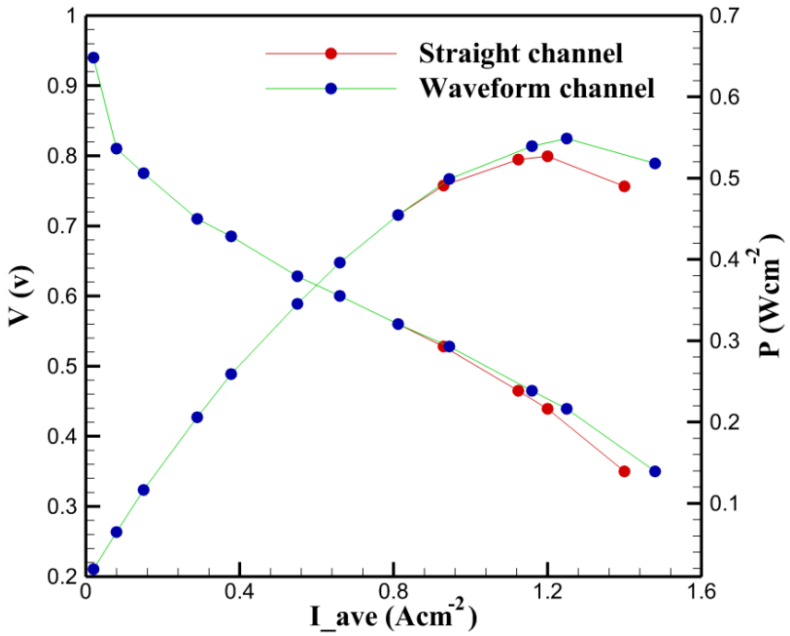

Fig. 8. The potential and power density along current density in the straight and waveform channel

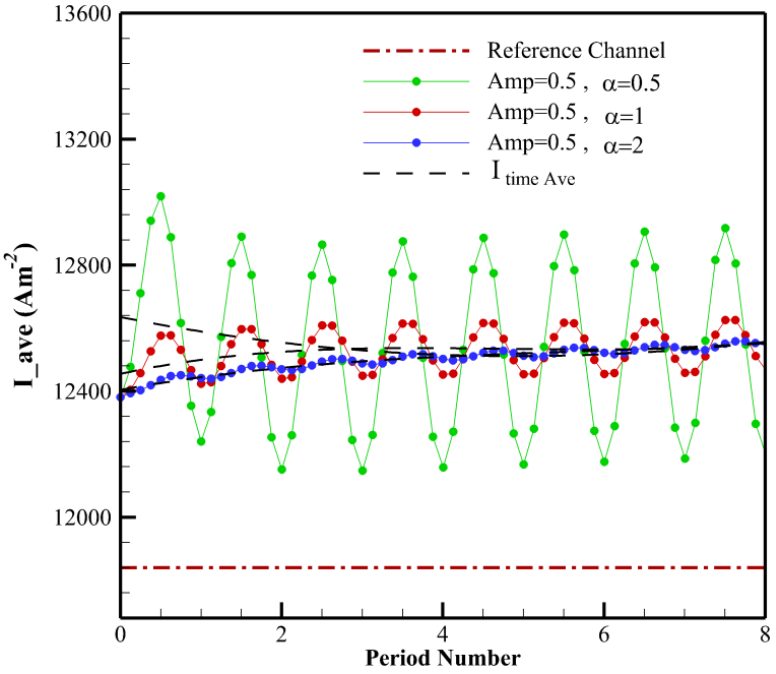

Fig. 9. The effect of the Womersley number α on the output current density versus time, with Amp=0.5, compared with the reference channel.

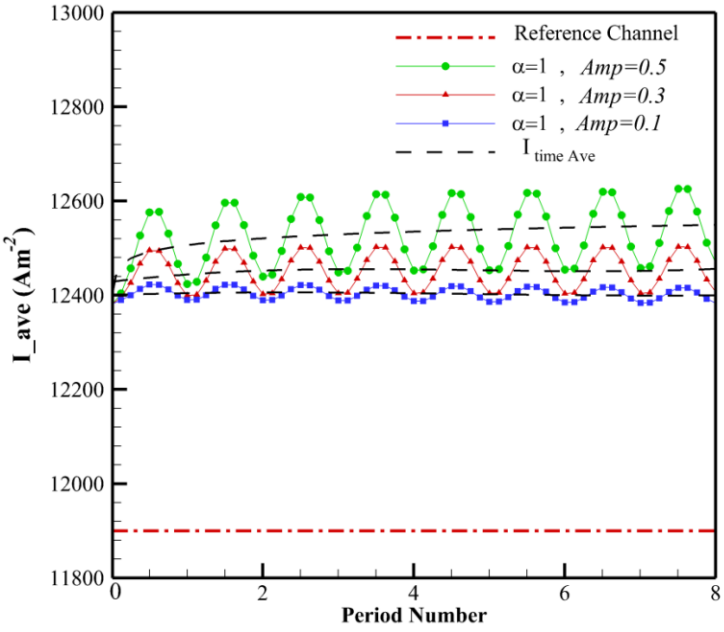

Fig. 10. The effect of pulsation amplitude on the average current density versus time for α =1.

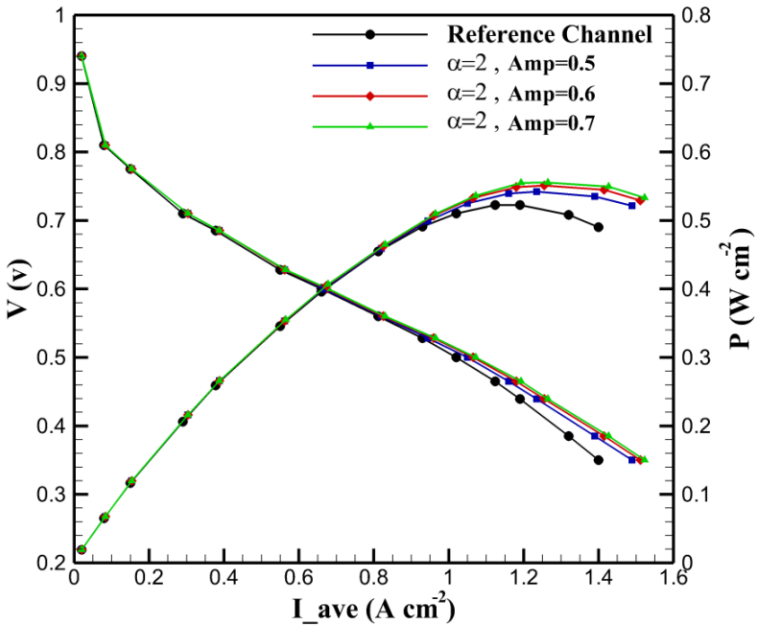

Fig. 11. The effect of larger values for *Amp* on potential and power density versus average current density at α =2.

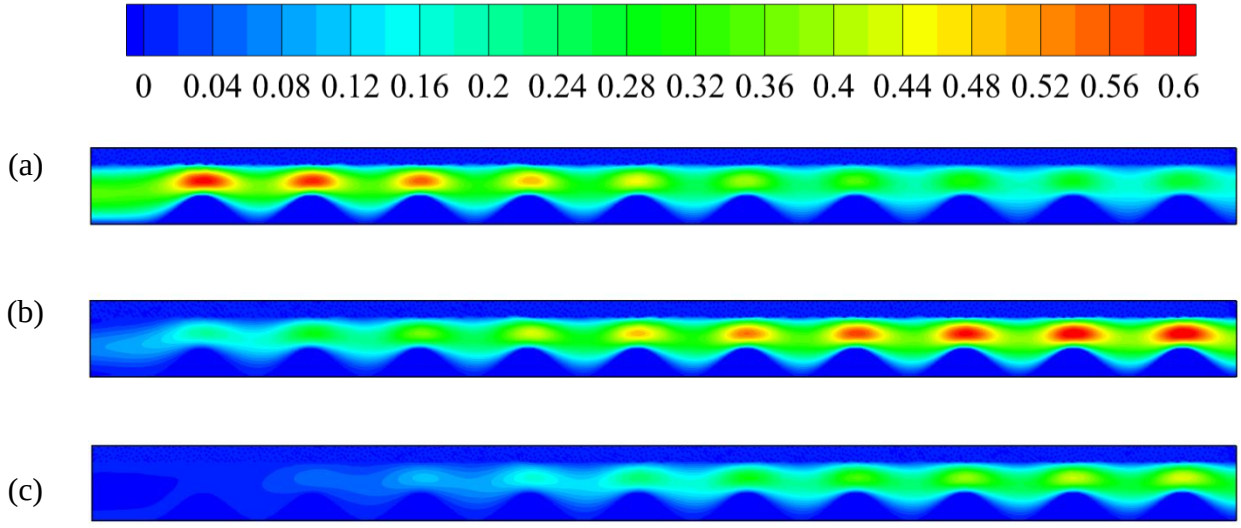

Fig. 12. Contours of velocity for α =2 and *Amp* =0.7 at different moments of time in a pressure pulsation period: at a) $t = T/4$, b) $t = T/2$, c) $t = 3T/4$.

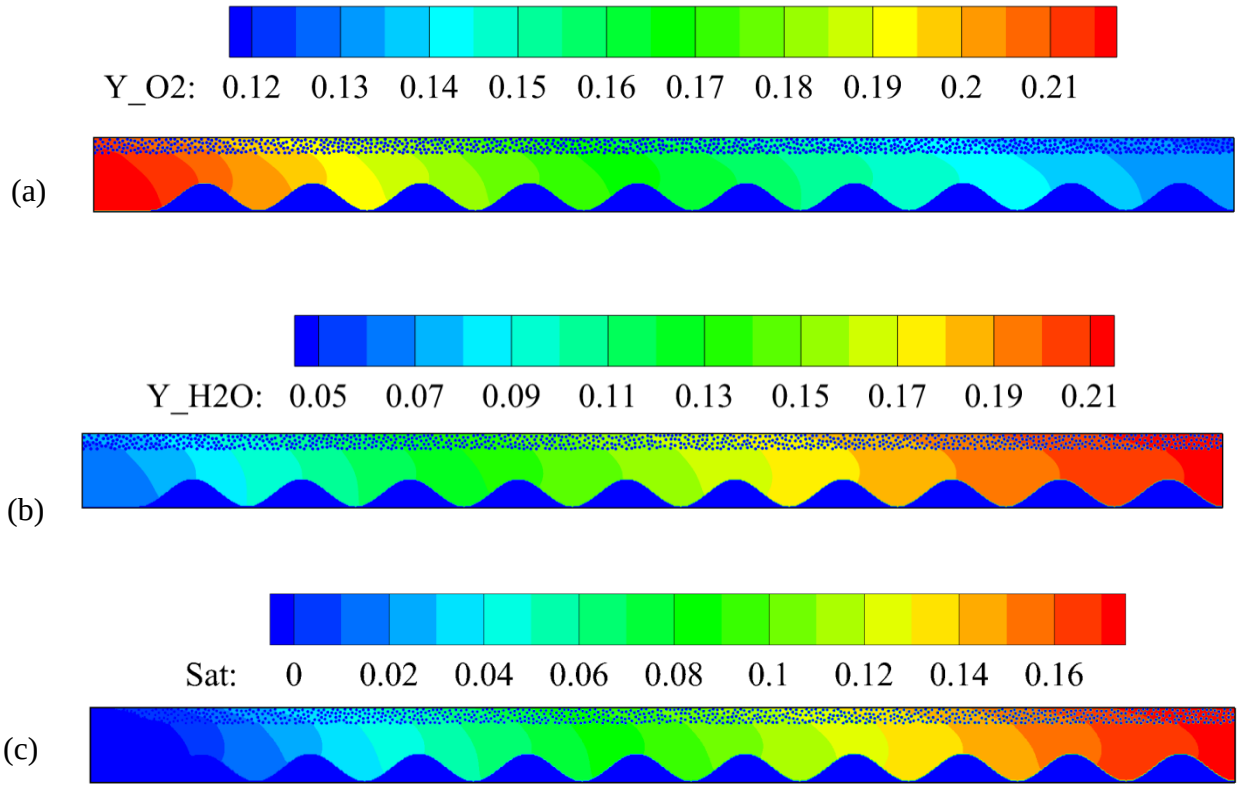

Fig. 13. The contours of (a) oxygen, (b) water vapor mass fraction, and (c) water saturation in the maximum power density case with pulsatile pressure with at α = 2 and Amp = 0.7 at time t = T/2.